Finite volume analysis of two-dimensional strain in a thick pipe with internal fluid pressure

S.R. Sabbagh-Yazdi, M.T. Alkhamis, M. Esmaili and N.E. Mastorakis

***Abstract*—**Internal fluid pressure of fluids may cause non-uniform distribution of stresses in thick pipes. In this work, a novel matrix free Unstructured Finite Volume Method based on Galerkin approach is introduced for solution of weak form of two dimensional Cauchy equilibrium equations of plane strain solid state problems on linear triangular element meshes. The developed shape function free Galerkin Finite Volume structural solver explicitly computes stresses and displacements in Cartesian coordinate directions for the two dimensional solid mechanic problems under either static or dynamic loads. The accuracy of the introduced algorithm is assessed by comparison of computed results of a thick pipe under internal fluid pressure load with analytical solutions. The performance of the solver is presented in terms of stress and strain contours as well as convergence behavior of the method.

Key-Words: Internal Fluid Pressure, Unstructured Finite Volume Method, Linear Triangular Element, 2D Strain, Thick Pipes

I. Introduction

Over the last decades a wide variety of numerical methods have been proposed for the numerical solution of partial differential equations. Among them the Finite Element Method (FEM) has firmly established itself as the standard approach for problems in Computational Solid Mechanics (CSM), especially with regard to deformation problems involving non-linear material analysis [1,2].

It is well known that numerical analysis of solids in incompressible limit could lead to difficulties. For example, fully integrated displacement based lower-order finite elements suffer from volumetric locking, which usually accompanies pressure oscillation in incompressible limit [3]. Also there are some difficulties for producing stiffness matrix and shape function in order to increase the convergence rate.

Although certain restrictions on mesh configuration had to be imposed to avoid locking, these restrictions were less severe than those of the equivalent FEM meshes.

The FVM developed from early finite difference techniques and has similarly established itself within the field of computational fluid dynamics (CFD) [4,1]. However, similar to the FEM, the FVM integrates governing equation(s) over pre-defined control volumes [2], which are associated with the elements making up the domain of interest and therefore, preserve the conservation properties of the equations. Although, the Finite Volume Method (FVM) was originally developed for fluid flow and heat and mass transfer calculations [6], recently, it is generalized for stress analysis in isotropic linear and non-linear solid bodies. Therefore, the interest for FVM application to the structural analysis problems involving incompressible materials has grown during the recent years. From the results of several benchmark solutions, the FVM appeared to offer a number of advantages over equivalent finite element models. For instant it can be stated that, unlike the FDM solution, FVM solution is conservative and incompressibility is satisfied exactly for each discretized sub-domain (control volume) of the computational domain [5].

In principle, because of the local conservation properties the FVMs should be in a good position to solve such problems effectively. Furthermore, numerical calculation with meshes consisting of triangular cells showed excellent agreement with analytical results. Meshes consisting of quadrilateral FVM cells displayed too stiff behavior, indicating a locking phenomenon [4]. Therefore, a number of researchers have applied FVMs to problems in CSM over the last decade [6,7] and it is now possible to classify these methods into two approaches, cell-centered and vertex-based ones.

In this paper, the explicit approach introduced is based on Galerkin approach with a kind of matrix free vertex base FVM on meshes of linear triangular elements. The accuracy of the introduced method is assessed by comparison of computed stresses and displacements for a thick pipe with internal fluid pressure load with analytical solutions and the performance of the solver is demonstrated in terms of stress and strain contours as well as convergence behavior of the method to the steady state condition.

Manuscript received January 3, 2008: Revised version received May 2, 2008

Saeed-Reza Sabbagh Yazdi, Associate Professor, of KNToosi University of Technology, Civil Engineering Department, No.1346 Valiasr Street, 19697-Tehran, IRAN SYazdi@kntu.ac.ir (Tel: 0098 21 88779473-5, Fax: 0098 21 88779476)

Mohamad T. Alkhamis, Assistant Professor of Civil Engineering Department, College of Technological Studies (Kuwait) P.O.Box: 39199 Nuzha, 73052 KUWAIT (E-mail: malkhamis@hotmail.com)

Mehdi Esmaili, Graduate Student, KN Toosi University of Technology, Civil Engineering Department, No.1346 Valiasr Street, 19697- Tehran, IRAN Mehdiesma@gmail.com

Nikos E. Mastorakis, is Professor of Military Institutes of University Education (ASEI) Hellenic Naval Academy, Terma Chatzikyriakou 18539,Piraues, GREECE

II. Mathematical Model

The universal law governing any continuum undergoing motion is given by general form of Cauchy's equilibrium equations:

$$\rho\ddot{u} = S^T\sigma + b \tag{1}$$

Where σ is the stress tensor, b is the body force, ρ is the material density and $\ddot{u}$ is the acceleration.

For two dimensional problems, $\vec{u} = (u_x, u_y)^T$ is the displacement vector and $\sigma = (\sigma_{xx}, \sigma_{yy}, \sigma_{xy})^T$ is tensor vector. The operator S^T for two-dimensional problems is defined as,

$$S^T = \begin{bmatrix} \frac{\partial}{\partial x} & \circ & \frac{\partial}{\partial y} \\ \circ & \frac{\partial}{\partial y} & \frac{\partial}{\partial x} \end{bmatrix}$$

So, the matrix form of Cauchy equations for two-dimensional problems is:

$$\rho\begin{Bmatrix} \frac{\partial^2 u_x}{\partial t^2} \\ \frac{\partial^2 u_y}{\partial t^2} \end{Bmatrix} = \begin{bmatrix} \frac{\partial}{\partial x} & \circ & \frac{\partial}{\partial y} \\ \circ & \frac{\partial}{\partial y} & \frac{\partial}{\partial x} \end{bmatrix}\begin{Bmatrix} \sigma_{xx} \\ \sigma_{yy} \\ \sigma_{xy} \end{Bmatrix} + \begin{Bmatrix} b_x \\ b_y \end{Bmatrix} \tag{2}$$

For stress-strain relationship, the common Hook equation can be used as,

$$\sigma = D\varepsilon \tag{3}$$

Where D is the constitutive property matrix and for plane strain problems is:

$$D = \begin{bmatrix} 1 & \frac{\upsilon}{1-\upsilon} & \circ \\ \frac{\upsilon}{1-\upsilon} & 1 & \circ \\ \circ & \circ & \frac{1-2\upsilon}{2(1-\upsilon)} \end{bmatrix} \times \frac{E(1-\upsilon)}{(1+\upsilon)(1-2\upsilon)}$$

Here, υ is the Poison ratio and E is the Young modules of elasticity. So the Cauchy's equilibrium equations in two Cartesian coordinate directions can be written as:

$$\begin{aligned} \rho\frac{\partial^2 u_x}{\partial t^2} &= \frac{\partial}{\partial x}\left(C_1\frac{\partial u_x}{\partial x} + C_2\frac{\partial u_y}{\partial y}\right) + \frac{\partial}{\partial y}C_3\left(\frac{\partial u_x}{\partial y} + \frac{\partial u_y}{\partial x}\right) + b_x \\ \rho\frac{\partial^2 u_y}{\partial t^2} &= \frac{\partial}{\partial x}C_3\left(\frac{\partial u_x}{\partial y} + \frac{\partial u_y}{\partial x}\right) + \frac{\partial}{\partial y}\left(C_2\frac{\partial u_x}{\partial x} + C_1\frac{\partial u_y}{\partial y}\right) + b_y \end{aligned} \tag{4}$$

Where for plane strain problems:

$$C_1 = \frac{E(1-\upsilon)}{(1+\upsilon)(1-2\upsilon)}, \quad C_2 = \frac{E\upsilon}{(1+\upsilon)(1-2\upsilon)}, \quad C_3 = \frac{E}{2(1+\upsilon)}$$

III. Numerical Formulation

In order to obtain the discrete form of the Cauchy's equation in *i* direction, the following form is used:

$$\rho\frac{\partial^2 u_i}{\partial t^2} = \frac{\partial \sigma_{ij}}{\partial x_i} + b_i \qquad (j = 1,2) \tag{5}$$

In which the stresses are defined as:

$$\sigma_{11} = \left(C_1\frac{\partial u_x}{\partial x} + C_2\frac{\partial u_y}{\partial y}\right), \quad \sigma_{12} = C_3\left(\frac{\partial u_x}{\partial y} + \frac{\partial u_y}{\partial x}\right)$$

$$\sigma_{21} = C_3\left(\frac{\partial u_x}{\partial y} + \frac{\partial u_y}{\partial x}\right), \quad \sigma_{22} = \left(C_2\frac{\partial u_x}{\partial x} + C_1\frac{\partial u_y}{\partial y}\right)$$

By application of the Variational Method, after multiplying the residual of the above equation by the test function ω and integrating over a sub-domain Ω (Figure 1), in the absence of body forces we have,

$$\int_\Omega \omega.\rho\frac{\partial^2 u_i}{\partial t^2}d\Omega = \int_\Omega \omega.(\vec{\nabla}.\vec{F}_i)d\Omega \tag{6}$$

Where, i direction stress vector is defined as $\vec{F}_i = \sigma_{i1}\hat{i} + \sigma_{i2}\hat{j}$.

The terms containing spatial derivatives can be integrated by part over the sub-domain Ω and then equation 6 may be written as,

$$\int_\Omega \omega.\rho\frac{\partial^2 u_i}{\partial t^2}d\Omega = [\omega.\vec{F}_i]_\gamma - \int_\Omega(\vec{F}_i.\vec{\nabla}\omega)d\Omega \tag{7}$$

According to the Galerkin method, the weighting function ω can be chosen equal to the interpolation function ϕ. In finite element methods this function is systematically computed for desired element type and called the shape function. For a triangular type element (with three nodes), the linear shape functions, ϕ_k, takes the value of unity at desired node *n*, and zero at other neighboring nodes *k* of each triangular element (Figure 2):

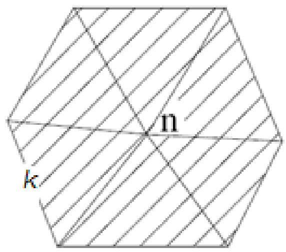

Fig.1 Sub-domain with area Ω_n

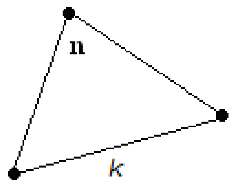

Fig.2. A linear triangular element

Therefore, the summation of the term $[\omega.\vec{F}_i]_\gamma$ over the boundary of the sub-domain Ω_n is zero.

The right hand side (RHS) of the equation (7) can be discretized as:

$$\int_\Omega (\vec{F}_i.\vec{\nabla}\phi)d\Omega \approx -\frac{1}{2}\sum_{k=1}^{N}(\tilde{F}_i\vec{\Delta l})_k \tag{8}$$

Where $\overrightarrow{\Delta l_k}$ is normal vector of the side k opposite to the node n and $\tilde{F}_i$ is the i direction piece wise constant stress vector at the centre of element associated with the boundary side k (inside the sub-domain Ω_n with N boundary sides)

For a sub-domain formed by linear triangular elements sharing node n, the left hand side (LHS) of the equation (7) can be written in discrete form as:

$$\frac{\partial^2}{\partial t^2}\left(\int_\Omega \phi u_i \, d\Omega\right) \approx \frac{\Omega_n}{3}\frac{d^2 u_i}{dt^2} \tag{9}$$

A finite difference approach is applied for discretizaton of the time derivative of i direction displacement, u_i. Hence, the LHS of equation (7) can be written as,

$$\rho\frac{\Omega_n}{3}\frac{d^2u_i}{dt^2} = \rho\left(\frac{u_i^{t+\Delta t} - 2u_i^t + u_i^{t-\Delta t}}{(\Delta t)^2}\right)\frac{\Omega_n}{3} \tag{10}$$

The final discrete form the equation (7) is obtained as,

$$\left(\frac{u_i^{t+\Delta t} - 2u_i^t + u_i^{t-\Delta t}}{(\Delta t)^2}\right) = \frac{3}{2\rho\Omega_n}\sum_{k=1}^{N}(\tilde{\sigma}_{i1}\Delta y - \tilde{\sigma}_{i2}\Delta x)_k \tag{11}$$

Considering direction $i=1$ as x an $i=2$ as y, the stresses $\tilde{\sigma}_{i1}$, $\tilde{\sigma}_{i2}$ are computed as,

$$\begin{aligned}
\tilde{\sigma}_{xx} &= \left\{C_1\frac{\partial u_x}{\partial x} + C_2\frac{\partial u_y}{\partial y}\right\} \approx \left\{\frac{1}{A_k}\sum_{m=1}^{3}(C_1u_x\Delta y - C_2u_y\Delta x)_m\right\} \\
\tilde{\sigma}_{xy} = \tilde{\sigma}_{yx} &= \left\{C_3\left(\frac{\partial u_x}{\partial y} + \frac{\partial u_y}{\partial x}\right)\right\} \approx \left\{\frac{1}{A_k}\sum_{m=1}^{3}(C_3u_x\Delta y - C_3u_y\Delta x)_m\right\} \\
\tilde{\sigma}_{yy} &= \left\{C_2\frac{\partial u_x}{\partial x} + C_1\frac{\partial u_y}{\partial y}\right\} \approx \left\{\frac{1}{A_k}\sum_{m=1}^{3}(C_2u_x\Delta y - C_1u_y\Delta x)_m\right\}
\end{aligned} \tag{12}$$

Where A_k is the area of triangular element (with $m=3$ sides) associate with boundary side k of the sub-domain Ω_n (Figure 3):

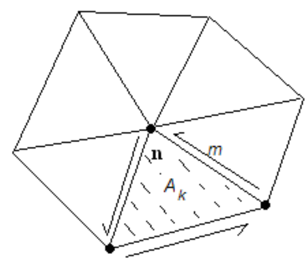

Fig.3: Triangular element with area A_k within the sub-domain Ω_n

IV. Computational Stepping

The time step Δt_n for each control volume can be computed as:

$$\Delta t_n \le \frac{r_n}{c} \tag{13}$$

Where c is wave velocity. According to the wave velocity, gained by equation (14):

$$c = \sqrt{\frac{E}{\rho(1-\upsilon^2)}} \tag{14}$$

Here, r_n is the average radius of equivalent circle that matches with the desired control volume ($r_n = \Omega_n / P_n$). For any control volume n this radius can be computed using area ($r = \Omega_n / \sum_{k=1}^{N_{edge}}(\Delta l)_k$) and perimeter ($P_n = \sum_{k=1}^{N_{edge}}(\Delta l)_k$) of the $2D$ control volume.

Due to the variations in sizes unstructured control volumes calculations, the allowable time step for computation of dynamic problems for the entire mesh is limited to the minimum associated with the smallest control volume of the domain. However, the large variation in grid size for the unstructured mesh will slow down the computations.

In present work, the local time step of each control volume is used for computation of static problems. In this technique to accelerate the convergence to steady state conditions, the computation of each control volume can advance using a pseudo time step which is calculated for its own control volume. The use of local time stepping greatly enhances the convergence rate.

V. COMPUTATIONAL RESULTS

In this section, the computational results of stress and strain analysis of a thick pipe under internal fluid pressure is presented. The numerical solution is performed by application of Galerkin finite volume method on an unstructured triangular mesh. The analytical solution is used to verify the results and satisfaction equality obtained. The model specifications are illustrated in Table.1.

The perpendicular normal vectors are computed on the nodes of the boundaries in order to impose the pressure load properly.

Table.1 Specification of a thick pipe

Parameters	Value
Young's modulus, E	21 MPa
Density, ρ	7850 kg/m^3
Poison ratio, υ	0.25
Interior radius	0.5
Outer radius	0.6
Interior Pressure	12000 Pa

Fig.4 shows the schematic view of the thick steel pipe with 12 kPa interior fluid pressure and zero outer pressure.

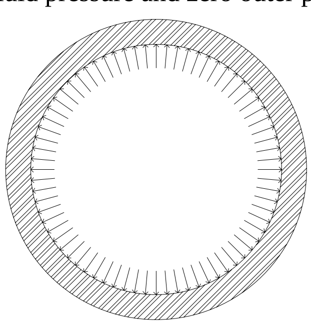

Fig.4 Thick Steel Cylinder under Pressure

In present computation, it is assumed that the cylinder is considerably long, and thus, the plain strain assumption is valid. For such a conditions radius stresses and tangential stresses from analytical solution are computed by (15), (16) equations from [8]:

$$\sigma_r = C_1 - \frac{C_2}{r^2} \qquad (15)$$

$$\sigma_t = C_1 + \frac{C_2}{r^2} \qquad (16)$$

Where r is the radius and C_1, C_2 are two coefficients which can be calculated by (17) and (18) equations:

$$C_1 = \frac{p_i r_i^{\,2} - p_o r_o^{\,2}}{r_o^2 - r_i^2} \qquad (17)$$

$$C_2 = \frac{(p_i - p_o) r_i^2 r_o^2}{r_o^2 - r_i^2} \qquad (18)$$

Here p_i, r_i are the interior pressure and interior radius respectively and p_o, r_o are the outer pressure and outer radius.

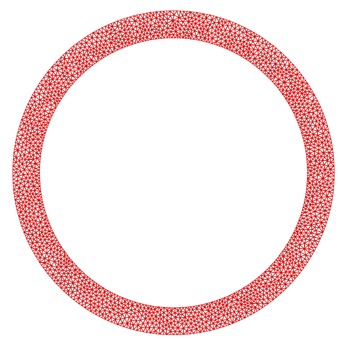

Fig.5 Unstructured Triangular Mesh

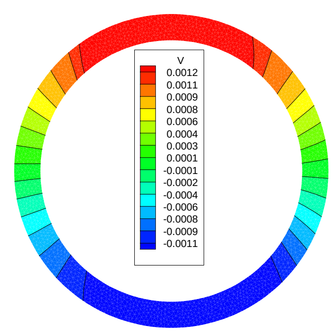

a) Vertical displacement

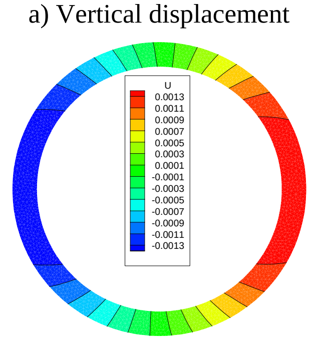

b) Horizontal displacement

Fig.6 Color coded maps of computed displacements

The unstructured triangular mesh utilized for the computation is presented in Fig.11. The unstructured triangular mesh is used for this purpose (Fig.5) with 2032 nodes and 3450 elements.

The displacement and stress contours are demonstrated in Fig. 6 and Fig.7.

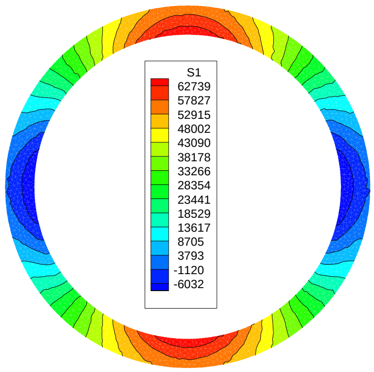

a) σ_{xx} stress

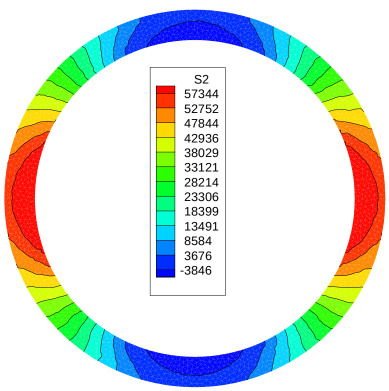

b) σ_{yy} stress

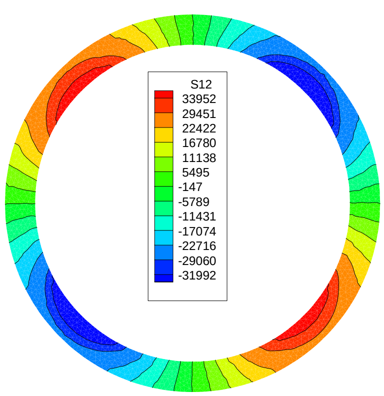

c) σ_{xy} stress

Fig.7 Color coded maps of computed stresses (Pa)

Section A-A which is used for comparison of computed results with the analytical solution is shown in Fig.8. The comparison of the computed radial stress with analytical solution along the thickness of the pipe is plotted in Fig.9. Convergence of the maximum strains to a constant value is plotted in Fig.10.

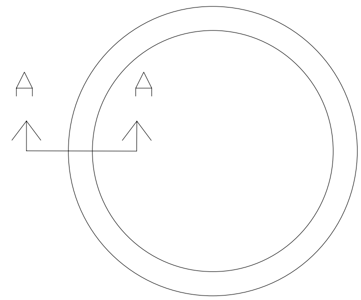

Fig.8 Location of section A-A

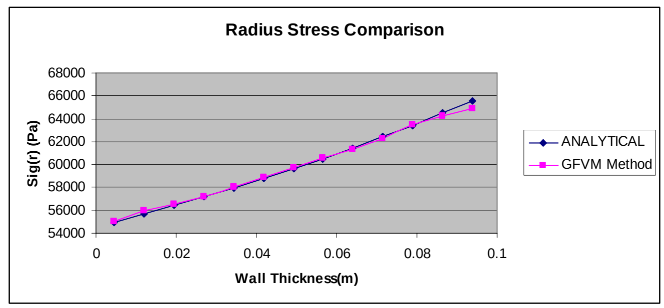

Fig.9 Horizontal displacement on section A-A

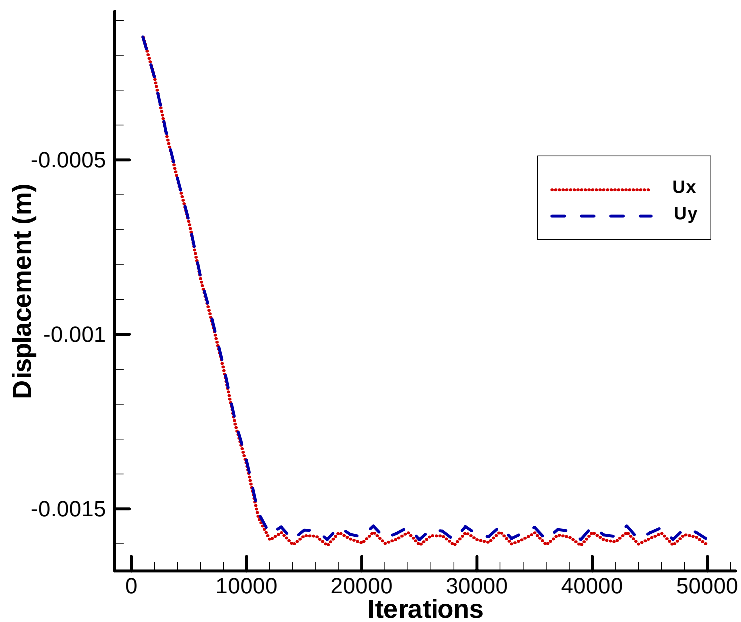

Fig.10 Converged results of displacement (on maximum point value)

VI. Conclusion

For analyzing the stresses and strains due to internal fluid pressure in thick pipes, a vertex base Galerkin Finite Volume method for explicit matrix free solution of two dimensional Cauchy equations is introduced in this paper. This computational model solves stress and deformation of solid mechanics under static and dynamic loads. The performance of described the computational solid mechanic algorithm is examined for various size of the meshes for a cantilever beam under a point load. Since there is no interpolation function in the numerical formulation of the present solver, the fine meshes provide more accurate results than the coarse meshes.

The present model is examined for some stress-strain in a thick pipe under fluid pressure. The comparison of the computed results with analytical solution presents promising agreements.

The new finite volume structural solver with light computational work load can easily be extended to three dimensions and be applied for solving large deformations of real world solid mechanics problems with arbitrarily curved geometries.

References

[[1] X. Lv, Y. Zhao, X.Y. Huang, G.H. Xia, X.H. Su, “A matrix-free implicit unstructured multigrid finite volume method for simulating structural dynamics and fluid–structure interaction”, *Journal of Computational Physics*, 2007 (to be appeared)

[2] O.C. Zienkiewicz, R.L. Taylor, “*The Finite Element Method Basic Formulation and Linear Problems*”, Vol.1, McGraw-Hill, Maidenhead, UK, 1989.

[3] I. Bijelonja , I. Demirdzˇic´, S. Muzaferija, “A finite volume method for incompressible linear elasticity” *Journal of Mechanical Engineering. 195, 2006, pp 6378–6390*

[5] C. Bailey, G.A. Taylor, M. Cross, P. Chow, “Discretisation procedures for multi-physics phenomena”, *Journal of Computational and Applied Mathematics 103, 1999, pp. 3-17*

[6] A.K. Slone, C. Bailey, M. Cross, “Dynamic solid mechanics using finite volume methods”, Old Royal Naval College, University of Greenwich, Applied Mathematical Modeling 27, 2003, pp 69–87

[7] I. Demirdzic, D. Martinovic, “Finite volume method for thermo-elasto-plastic stress analysis”, *Computer Methods in Applied Mechanics and Engineering 109, 199, pp. 331–349.*

[8] S.P. Timoshenko, J.N. Goodier, *Theory of Elasticity*, McGraw-Hill, New York, 1982.

First Author's biography may be found in:
http://sahand.kntu.ac.ir/~syazdi/
Nikos Mastorakis' biography may be found also in:
http://www.wseas.org/mastorakis